nature geoscience

SUPPLEMENTARY INFORMATION

DOI: 10.1038/NGEO2932

In the format provided by the authors and unedited.

River piracy and drainage basin reorganization led by climate-driven glacier retreat

Daniel H. Shugar, John J. Clague, James L. Best, Christian Schoof, Michael J. Willis, Luke Copland and Gerard H. Roe

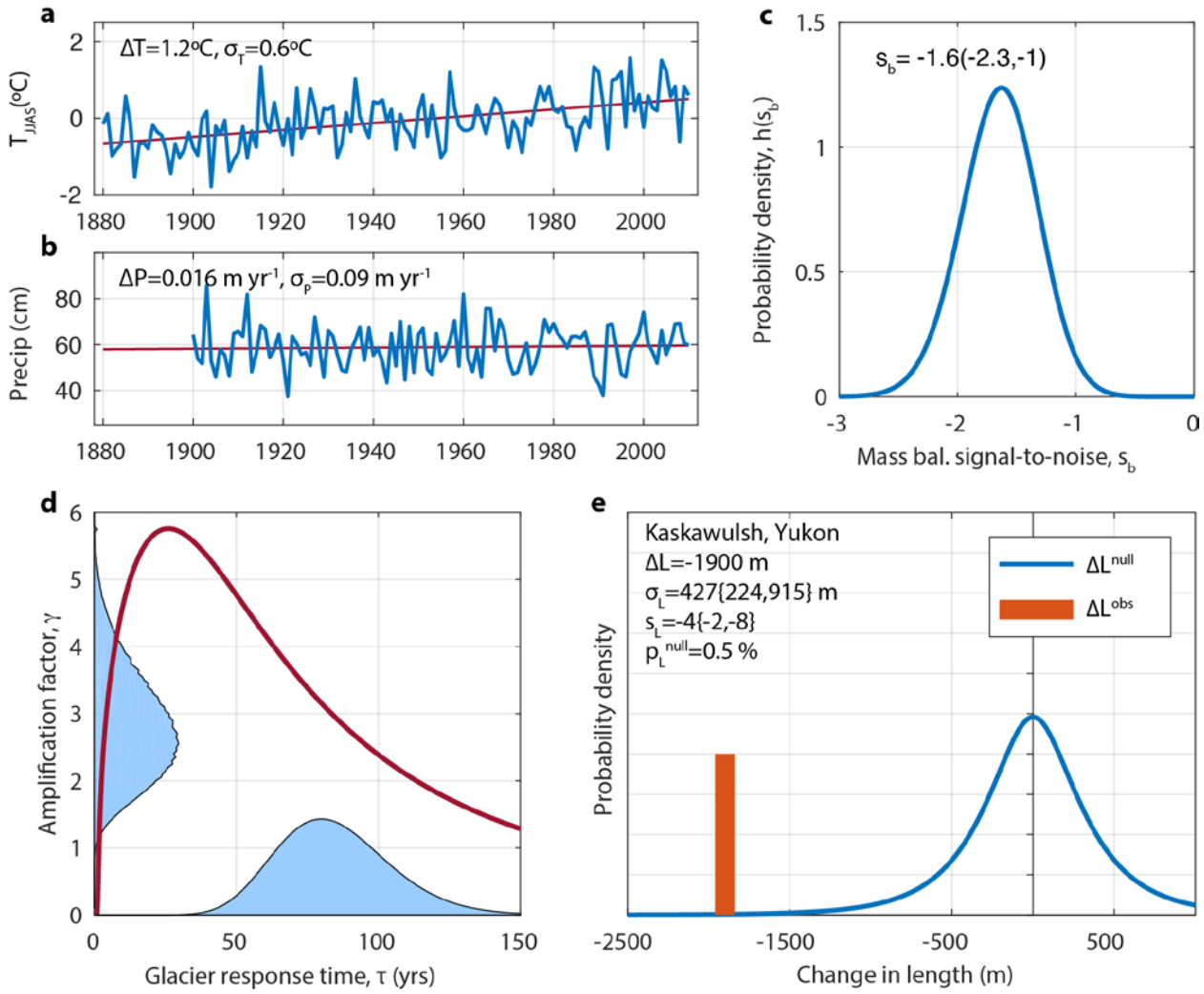

Figure S1. Analysis of climate trends and Kaskawulsh Glacier retreat (1880-2010), following the procedure outlined in Roe et al.[12]. **a**. Melt season surface temperature derived from the Berkeley Earth gridded dataset[1], and least-squares best-fit linear trend. **b**. same as **a**, but for annual mean precipitation obtained from Legates and Wilmott[2] with the trend extrapolated to 1880. **c**. Modeled probability density function (PDF) of the signal-to-noise ratio of mass balance, showing the median and 95% bounds. **d.** Relationship between glacier response time, τ, and the amplification factor, γ, for a 130-yr trend; the red curve shows the relationship between τ and γ; the blue shading on the x-axis shows the PDF for τ and the blue shading on the y axis shows the PDF of γ, that results from τ being projected onto the y axis via the red line. **e**. PDF for the change in length of Kaskawulsh Glacier, ΔL, in any 130-yr period with no climate change, compared with the observed retreat represented by the vertical red bar.

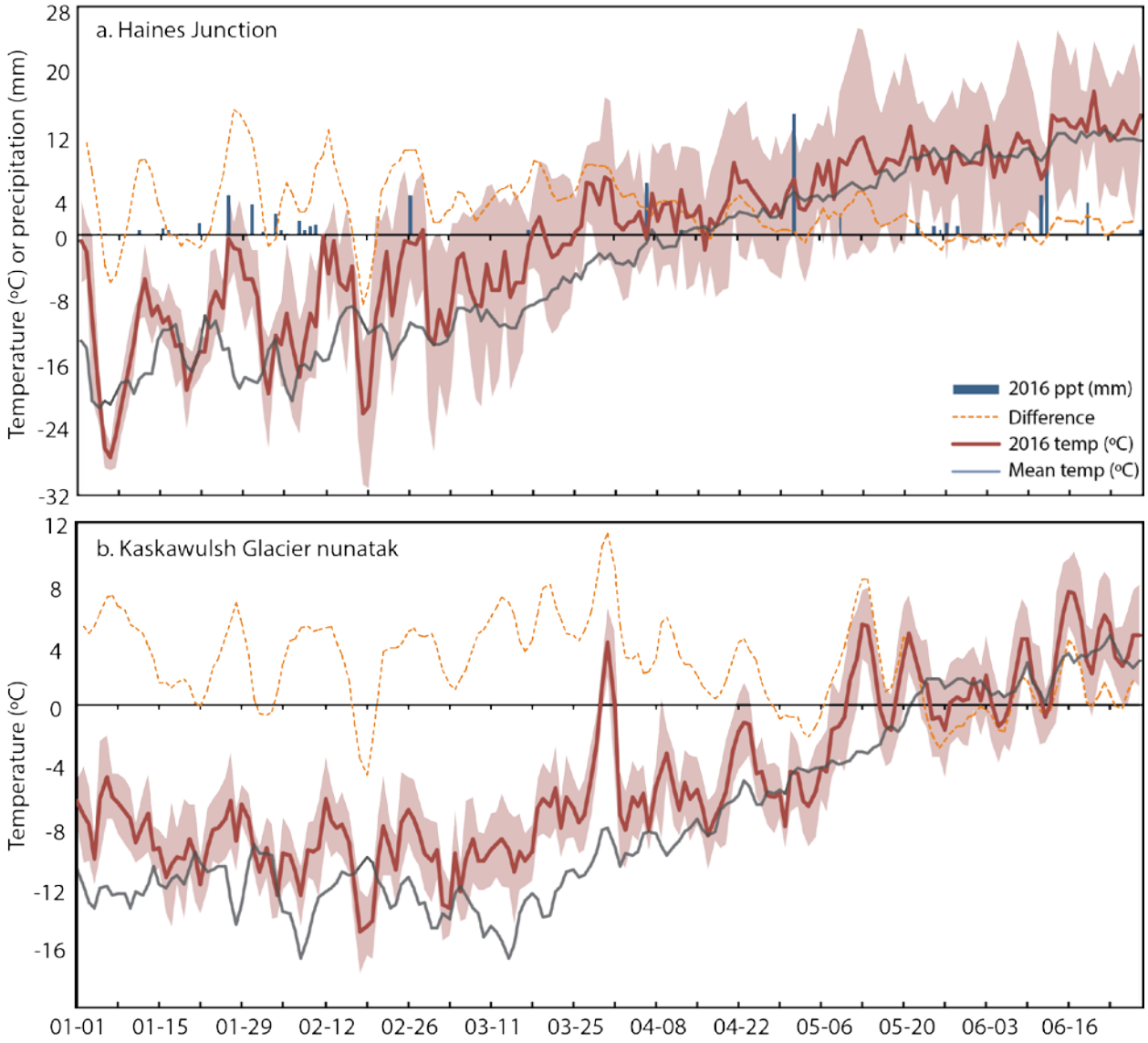

Figure S2. 2016 meteorological measurements from a. Haines Junction (Environment Canada station 2100630) and b. Kaskawulsh Glacier nunatak. At Haines Junction, both precipitation and air temperature are recorded, whereas at the nunatak, only air temperature is recorded. The pink shaded envelope represents the minimum and maximum recorded temperatures for each day in 2016.

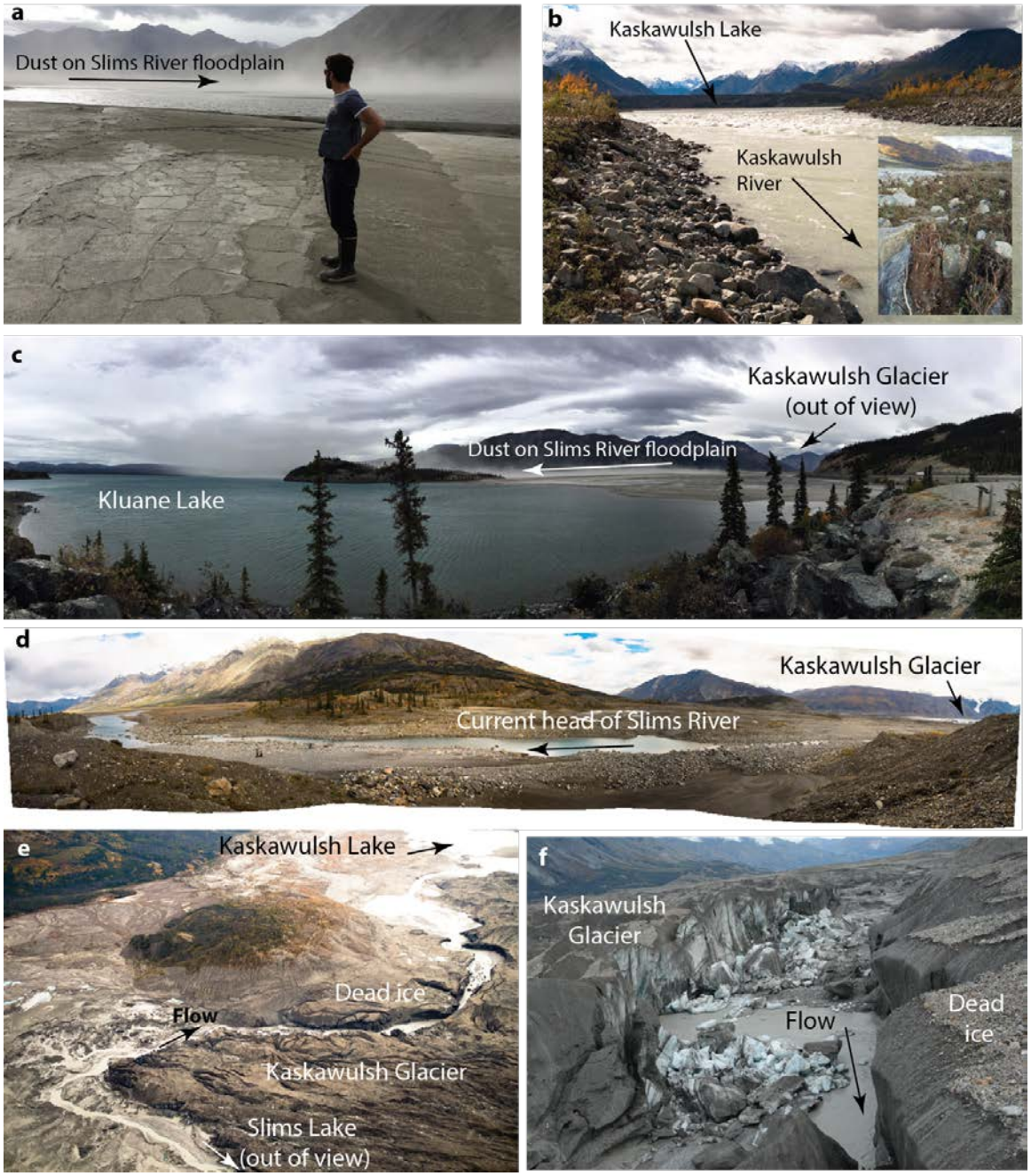

Figure S3. Photos of field area. **a**. Dust storm on Slims River delta with person for scale. **b**. Outlet of Kaskawulsh Lake and Kaskawulsh River with inset of ripped-up root mats caught on boulders and shrub willows. The highest of these root mats was observed 2 m above the river water surface level on September 2, 2016, indicating flood waters were at least that high during peak flows. A flood-deposited sand veneer also covered the banks. **c**. Dust storm on Slims River delta viewed from the north side of Kluane Lake. **d**. Panorama of the current head of Slims River flowing right to left. **e**. Aerial view of the terminus of Kaskawulsh Glacier showing the canyon connecting Slims Lake (out of view at bottom of frame) to Kaskawulsh Lake. Note the presence of dead ice on the downglacier side of the canyon, abutting the hill. **f**. Close-up aerial view of the canyon from described in **e** but facing upstream.

Table S1. List of satellite images used in the analysis.

Sensor	Satellite granule ID	Date of imagery
Landsat-1	LM10670171972246AAA02	09-02-1972
Landsat-2	LM20670171980177PAC00	06-25-1980
Landsat-5	LM50620171990201PAC00	07-20-1990
Landsat-7	LE70620172000189AGS00	07-09-2000
Landsat-7	LE70610182010257EDC00	09-14-2010
Landsat-8	LC80620172015142LGN00	07-25-2015
Landsat-8	LC80610172016170LGN00	06-18-2016
Landsat-8	LC80610172016186LGN00	07-04-2016
SPOT-5	SPOT5_HRG2_XS_20150814_N1_TUILE_SlimsRiver CanadaD0000B0000	08-14-2015
WorldView-1	WV01_20121029_102001001D5D0B00	10-29-2012
WorldView-1	WV01_20121029_102001001E70E600	10-29-2012

Supplementary References

1. Rohde, R., *et al.* A new estimate of the average earth surface land temperature spanning 1753 to 2011. *Geoinfor. Geostat.*, **1**, doi:10.4172/2327-4581.1000101 (2012).

2. Legates, D. R., Willmott, C. J. Mean seasonal and spatial variability in gauge corrected global precipitation. *Intl. J. Clim.*, **10**, 111-127 (1990).